

# We are IntechOpen, the world's leading publisher of Open Access books Built by scientists, for scientists

7,000

Open access books available

186,000

International authors and editors

200M

Downloads

Our authors are among the

154

Countries delivered to

TOP 1%

most cited scientists

12.2%

Contributors from top 500 universities



WEB OF SCIENCE™

Selection of our books indexed in the Book Citation Index  
in Web of Science™ Core Collection (BKCI)

Interested in publishing with us?  
Contact [book.department@intechopen.com](mailto:book.department@intechopen.com)

Numbers displayed above are based on latest data collected.  
For more information visit [www.intechopen.com](http://www.intechopen.com)



---

# Direction Controlled Growth of Organic Single Crystals by Novel Growth Methods

---

M. Arivanandhan, V. Natarajan,  
K. Sankaranarayanan and Y. Hayakawa

Additional information is available at the end of the chapter

<http://dx.doi.org/10.5772/53037>

---

## 1. Introduction

The green lasers are attractive and highly useful for lot of practical applications. It is more than fifty times brighter when compared to a red laser and thus it can be seen from miles away. Due to these features, the green lasers can be used in high-tech weapons for aiming purposes. Moreover, the green lasers are highly useful for laser televisions and medical applications. Most of the commercially available green lasers are based on the diode pumped solid state frequency-doubled (DPSSFD) laser technology. For the past several decades, researchers and several industries were trying to develop the laser diodes based on the compound semiconductors such as Gallium nitride (GaN) and Indium Gallium nitride (InGaN) especially in the blue and green region of wavelengths [1]. However, it is very difficult to grow bulk crystal of these materials with reasonable quality. Moreover, for the preparation of epitaxial thin films of these materials on substrates, highly sophisticated and expensive techniques like molecular beam epitaxy (MBE) and metal organic chemical vapour deposition (MOCVD) are needed. Apart from these growth aspects, the relatively low power and limited wavelength range restricts their use in important applications [2]. Therefore, laser sources based on Second harmonic generation (SHG) is a better choice for the applications which requires higher powers or longer wavelengths (>400nm). As a consequence, the green laser technology still depends on the nonlinear optical phenomena such as frequency doubling.

In the DPSSFD lasers, a nonlinear optical (NLO) crystal must be placed to halves the wavelength of a solid state laser. In the today's market, inorganic NLO crystals of Potassium Titanyl Phosphate (KTP), Lithium triborate (LBO) are used as frequency doublers. For example, the KTP crystal is used to generate green laser at 532 nm by halving the wavelength of Nd:YAG laser of 1064nm. Organic NLO materials are superior to the inorganic materials both in the speed

of response and high NLO susceptibilities. Moreover, they have high laser damage threshold compared to inorganic materials. For frequency doubling applications, the growth direction of NLO crystal has to be controlled towards a phase-matched direction. Therefore, direction-controlled growth is an indispensable technology, especially for the bulk growth of NLO crystals due to its anisotropic nature of NLO properties.

In the literature, different kind of direction-controlled growth technique such as indirect laser heated pedestal growth (ILHPG) method [3], Microtube-Czochralski ( $\mu$ T-CZ) method [4], seed-oriented undercooled melt growth [5], Vertical Bridgman (VB) method [6], and uniaxially solution crystallization (USC) method of Sankaranarayanan-Ramasamy [7] have been reported with the aim of growing unidirectional NLO crystals. Despite the unidirectional organic NLO crystal can be grown by ILHPG [3] and seed-oriented undercooled melt growth [5], the complicated experimental set-up and multistep growth process leads to difficulty in growing large size unidirectional crystal. Whereas the  $\mu$ T-CZ [4] and VB [6] methods are more versatile and bulk directional crystals can be grown by optimizing the growth parameters. On the other hand, the recently reported USC method [7] attracted the researchers by its unique advantage than the other methods such as unidirectional growth at ambient temperature which causes minimum thermal induced grown-in defects using simple experimental set-up with high solute-crystal conversion efficiency and high growth rate.

Benzophenone is a promising organic NLO material and it has nearly six times higher NLO efficiency than that of Potassium dihydrogen phosphate (KDP), a well-known inorganic NLO material [8, 9]. It crystallizes in the non-centrosymmetric orthorhombic space group  $P2_12_12_1$  and the lattice parameters are reported as  $a = 10.26 \text{ \AA}$ ,  $b = 12.09 \text{ \AA}$  and  $c = 7.88 \text{ \AA}$  [10]. Benzophenone is also known as aromatic ketone which is a particularly interesting material for studying the impact of crystallization conditions on crystal defects and quality [11]. In the present investigation, benzophenone single crystals have been grown by VB,  $\mu$ T-CZ and USC method. Since all the three growth methods are quite different, the crystals grown by these methods may have different crystalline perfection, which may lead to some differences in their physical properties. In order to understand the impact of crystallization conditions on crystal quality, a comparative study has been made on the benzophenone crystals grown by these three different techniques by employing X-ray diffraction (XRD), and high resolution X-ray diffraction (HRXRD).

Further, the USC growth method was extended to grow benzophenone single crystals in three different orientations. The growth rate of the crystal in different orientations were measured. Laser damage threshold and hardness of the directional samples were studied. In harmonic generation, the range of conversion is recently extended up to extreme ultraviolet and soft X-ray regions [12]. During the practical operation, the NLO materials are exposed to high intensity laser radiations for harmonic generations. Thus, the NLO crystals must have the ability to withstand high power laser radiations [13]. Laser induced damage studies on NLO crystals are obviously important, since the surface and bulk damage of the crystal by high power lasers limits its performance in NLO applications. The damage threshold of the NLO material must be investigated by multiple shot mode as well as single shot mode

since the NLO crystals are generally used for long durations in repetitive mode at various applications. On the other hand, mechanical hardness of a material is also one of the decisive properties especially for post-growth processes and device fabrications. Hence, the laser damage threshold and hardness properties of the unidirectional samples were investigated. The observed laser damage profile and hardness variations in three different growth directions are explained based on the crystal structure of benzophenone. The mechanism for the laser induced damage in benzophenone is discussed.

## 2. Experiment

### 2.1. VB growth of benzophenone crystal

Prior to filling the source material of benzophenone, the ampoules were chemically cleaned in HCl : HNO<sub>3</sub> mixture (prepared in the ratio of 1: 1) and kept in electronic grade acetone in order to remove the surface contamination to avoid any possible multi-heterogeneous nucleation. The benzophenone powder was purified by the zone refining method using a movable furnace assembly. Bulk crystals of benzophenone were grown using the indigenously constructed VB system (Figure 1). The VB system consists of three major parts such as transparent furnace, temperature controller and ampoule translation assembly. The transparent furnace consists a central quartz tube which is centrally placed in a glass beaker filled with two immiscible liquids. Sufficient volumes of deionized water and sunflower oil (normally used for cooking) were used for low temperature and high temperature zones respectively since the melting point of benzophenone is ~48°C. Spiral shaped tubular resistive heaters which are fabricated in our laboratory, were encircled the growth tube at hot and cold zones. Commercially bought Eurotherm 818 PID temperature controller with an accuracy of ±0.1°C was employed to control the zone temperatures. Lowering rate of 1-4 mm.h<sup>-1</sup> was achieved using an in-house built ampoule lowering system

Direct observation of solid-liquid interface, which is more feasible in transparent furnaces than conventional furnaces, is important for the directional solidification to determine the desired interface shape by controlling the growth parameters. In the case of VB growth of organic material, due to its low thermal conductivity one has to adopt the recommended translation rate of 1-2 mm.h<sup>-1</sup> [14]. With the aid of thermocouple attached ampoule holder, the in-situ thermal profile analysis was made during the growth and measured a vertical temperature gradient near the solid-liquid interface. In the present work, the growth run was initiated with the translation rate of 1 mm.h<sup>-1</sup> when hot and cold zone temperatures are kept at 55 and 32°C. The growth experiments were performed with different growth parameters and an experiment was successful with reasonably good quality crystals, when the hot and cold zone temperatures were 51°C and 35°C, respectively while the translation rate was 1 mm.h<sup>-1</sup>. Hence, the temperature gradient of the furnace and lowering rate of the ampoule influence the quality and directionality of the growing crystal. The more details of the growth processes can be found elsewhere [6].



**Figure 1.** Transparent vertical Bridgman growth system.

## 2.2. $\mu$ T-CZ growth of benzophenone crystals

A technical brief of the experimental setup employed in this investigation can be found elsewhere [4]. Highly purified benzophenone material was filled in a circular shape static glass crucible having the size of 60 mm ID and 110 mm height. The source material filled crucible was placed inside a resistive heated furnace. Commercially bought Eurotherm 818 PID temperature controller with an accuracy of  $\pm 0.1^\circ\text{C}$  was employed to control the temperature of the furnace. In the present work, instead of seeding by pre-grown defect free seed crystal, stainless steel microtube of size 8  $\mu\text{m}$  ID has been used for seeding the melt. Since melt wets the inner walls of the fine capillary tube, it rose to a height, which depended by the tube radius, the surface tension of the melt, the melt density and the contact angle of the melt with micro tube. A fine column of melt raised inside the microtube was crystallized first due to heat desipation through seed rod and the grown crystal inside the microtube was acted as a seed for further growth. The growth temperature and the pulling rate of the crystal were optimized for the growth of benzophenone single crystals. The optimized growth parameters for the present investigation are, pulling rate: 1.0 - 1.5  $\text{mm}\cdot\text{hr}^{-1}$ , seed rotation rate: 5-10 rpm, the cooling rate:  $1^\circ\text{C}\cdot\text{hr}^{-1}$ , length of the microtube underneath the melt surface ( $l_{ums}$ ): 1.5 mm and the axial thermal gradient:  $8^\circ\text{C}/\text{cm}$ . The temperature at which the microtube seeding is made ( $t_{ms}$ ), and  $l_{ums}$  play a vital role in deciding the orientation of the growing crystal

inside the microtube (will be discussed in the next section) [4]. Once the growth run was completed, the system temperature was reduced to room temperature (31°C) at a predefined cooling rate to avoid the thermal stress in the grown crystal.

### 2.3. Growth of benzophenone crystal by USC method

Unidirectional benzophenone single crystals have been grown along  $\langle 110 \rangle$  direction by mounting a dislocation free seed crystal at the bottom of a glass ampoule in such a way that the (110) plane of seed crystal facing towards the saturated solution of benzophenone. Then, the ampoule was filled with saturated solution of benzophenone having optimized solute concentration and porously sealed. The schematic view of the experimental set-up used for the USC growth is shown in Figure 2. The transparent nature of the experimental set-up and the visibility of the solid-liquid interface, facilitate the measurement of growth rate in the particular crystallographic direction. Growth rate of a uniaxial crystal of particular size along a particular growth axis largely depends on the packing density of that plane, purity of the raw materials, degree of supersaturation and the rate of diffusion of the solute in the solvent medium. A comprehensive experimental report can be found in the literature [15]. In USC method, since the crystal is growing in selective growth orientation, the commonly observed growth features in the case of conventional solution grown crystal such as growth sectors, grain boundaries, twins, stacking faults and dislocations are not observed in the X-ray topography [15], indicating that the USC grown sample is relatively free from these defects.

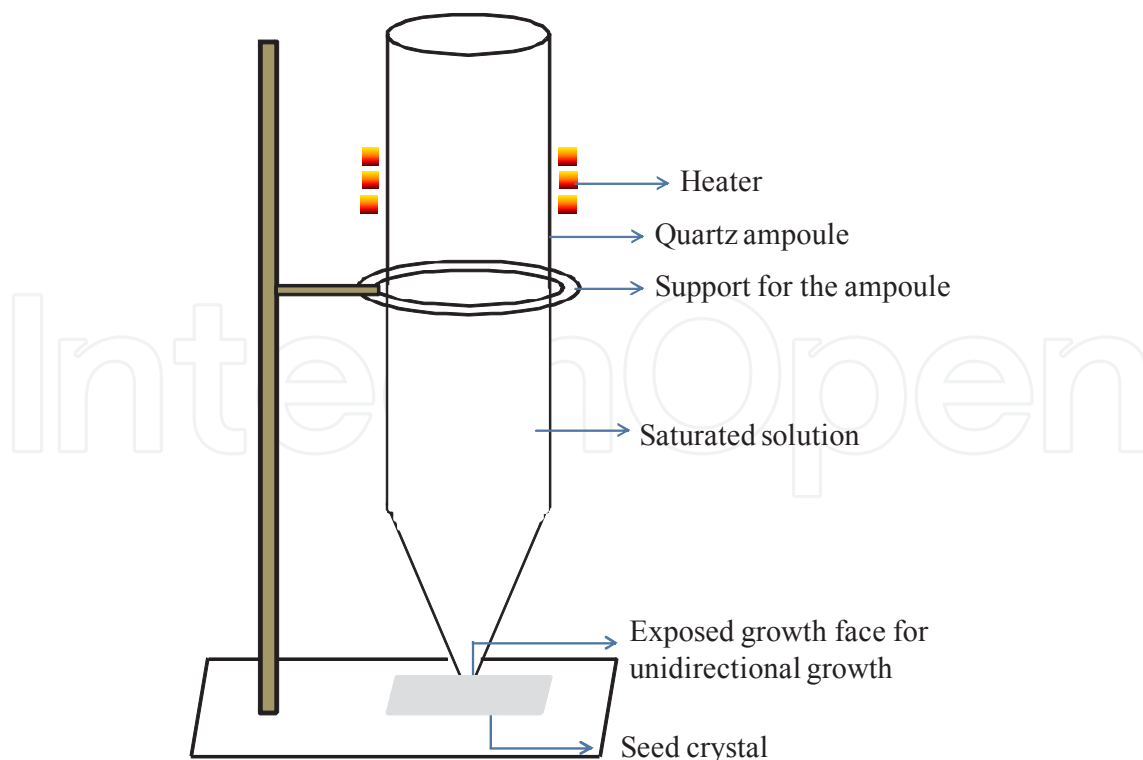


**Figure 2.** Schematic view of USC experimental set-up.

### 3. Results and discussion

#### 3.1. VB growth

The VB growth was conducted for various translation rate of ampoule and temperature gradient of the two zone furnace to control the quality of the crystal. The growth experiment was initiated with the translation rate of  $1 \text{ mm.h}^{-1}$  and the temperature gradient of  $0.75^\circ\text{C/mm}$ . The grown crystal was opaque with larger grains and cracks (Figure 3 a). The major cracks may be attributed due to low thermal conductivity of benzophenone. This result basically confirms the suitability of the thermal profile present in the constructed furnace for the Bridgman growth of benzophenone crystal. In order to study the effect of temperature gradient on the quality of grown crystal, the temperature gradient of the furnace was lowered to  $0.5^\circ\text{C/mm}$  by increasing the cold zone temperature. A single crystal with relatively high transparency, small numbers of cracks and few numbers of bubbles were obtained (Figure 3 b). Due to the transparency of the furnace and the melt, the solid-liquid interface was visible and found to be concave.

In an attempt to remove the grown-in defects such as cracks, bubbles and to study the influence of translation rate on these grown-in defects, the growth runs were made with the translation rate of 2 and  $2.5 \text{ mm.h}^{-1}$ . The observations made on the resultant material obtained from the growth run with the translation rate of  $2 \text{ mm.h}^{-1}$  revealed that the transparency of the ingot was increased when compared to the previous growth run and the number of large size cracks and bubbles was reduced. However, the concavity of the solid-liquid interface was maintained. Further increase in the translation rate to  $2.5 \text{ mm.h}^{-1}$ , resulted a bubble-free ingot with good transparency (Figure 3 c). However, very fine cracks were observed in the crystal possibly due to the thermally induced strain and faster growth rate at high translation rate. Also, the high translation rate increases the concavity of the solid-liquid interface.

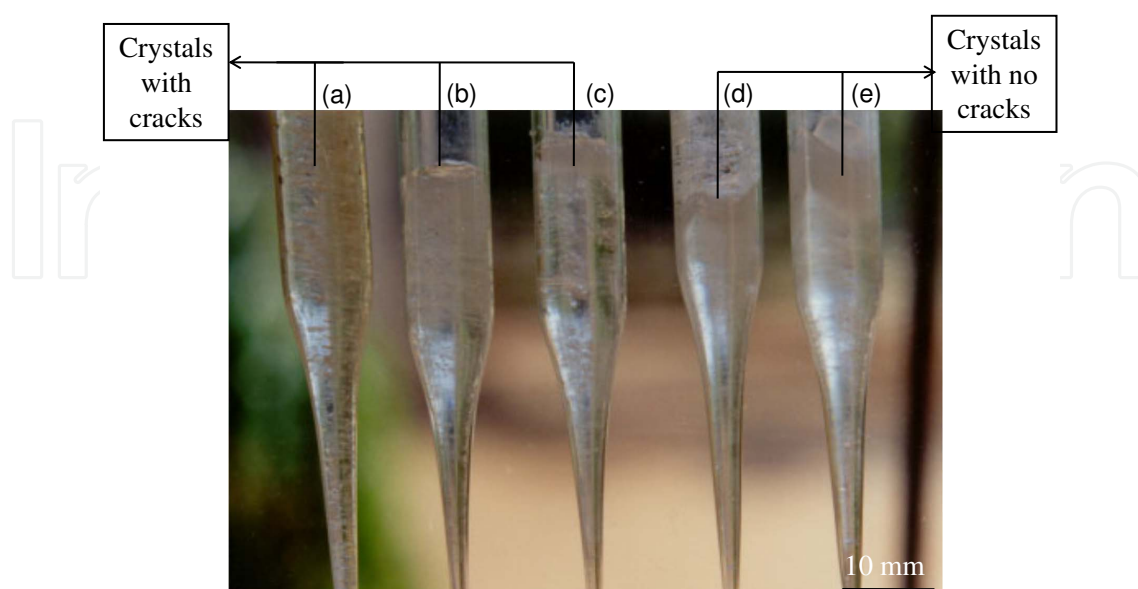


**Figure 3.** Photographs of the grown crystal in various growth runs.

Even though the obtained single crystal from the growth run conducted with the vertical temperature gradient of  $0.5^{\circ}\text{C}/\text{mm}$  and translation rate of  $2.5\text{ mm}\cdot\text{h}^{-1}$  was free of bubbles and larger cracks, the fine cracks due to thermally induced strains are present. To eliminate the fine cracks, the hot and cold zone temperatures were reduced from  $55$  to  $51^{\circ}\text{C}$  and  $39$  to  $35^{\circ}\text{C}$ , respectively. At this temperature, a growth run with the translation rate of  $1\text{ mm}\cdot\text{h}^{-1}$  has resulted a near flat solid-liquid interface but the grown single crystal was not free of fine cracks. Also, further reduction in the translation rate leads to supercooling of melt. Due to different thermal conductivity and viscosity of the liquids of two zones, a sharp variation of temperature was observed at the interface between the liquids. This variation probably causes the fine cracks in the grown crystal.

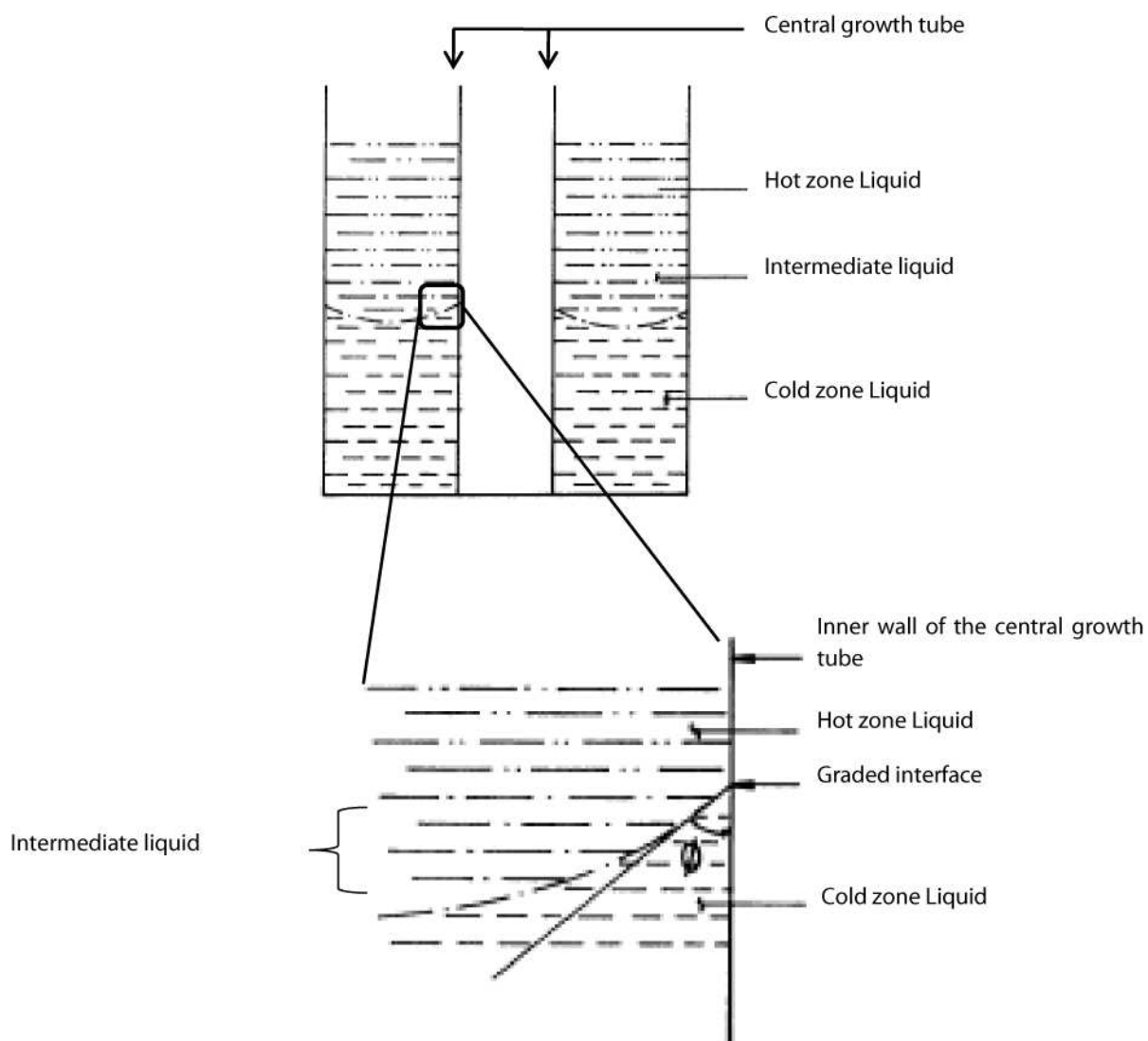


**Figure 4.** Schematic view of graded interface in VB system.

In order to control the fine cracks, a graded interface was established by introducing intermediate liquid in between the two liquids which has different wetting angle ( $\varphi$ ) with the in-

ner growth tube (Figure 4). The density of the intermediate liquid is smaller than the topper liquid and larger than the bottom one. It is expected that by establishing the graded interface, one can control the sharp variation of temperature at the interface between hot and cold zone thereby the fine cracks in the grown crystal. Keeping the zone temperatures and translation rate as constant, growth runs were conducted with different volumes (50, 100 and 150 mL) of intermediate liquid. The result shows that the grown in defects such as fine cracks were suppressed and a transparent, optical quality single crystalline ingot was grown when 150 mL of intermediate liquid was used. Figure 3 d, e illustrates the grown benzophenone ingots free of grown in defects such as thermal induced strains, cracks and bubbles.

### 3.2. Microtube CZ growth

The selection of microtube for the material to be grown as a bulk single crystal mainly depends on the melting point of the source material, surface tension of the melt, and the chemical reactivity of the melt with the microtube. In the present case, due to the low melting point of the benzophenone ( $\sim 48^\circ\text{C}$ ), stainless steel microtube (ID: 0.8 mm) was used for seeding the melt. The important experimental parameters used for controlling nucleation inside the tube are, radius and rotation rate of the microtube,  $t_{msr}$  pulling rate, axial temperature gradient and  $l_{ums}$ .

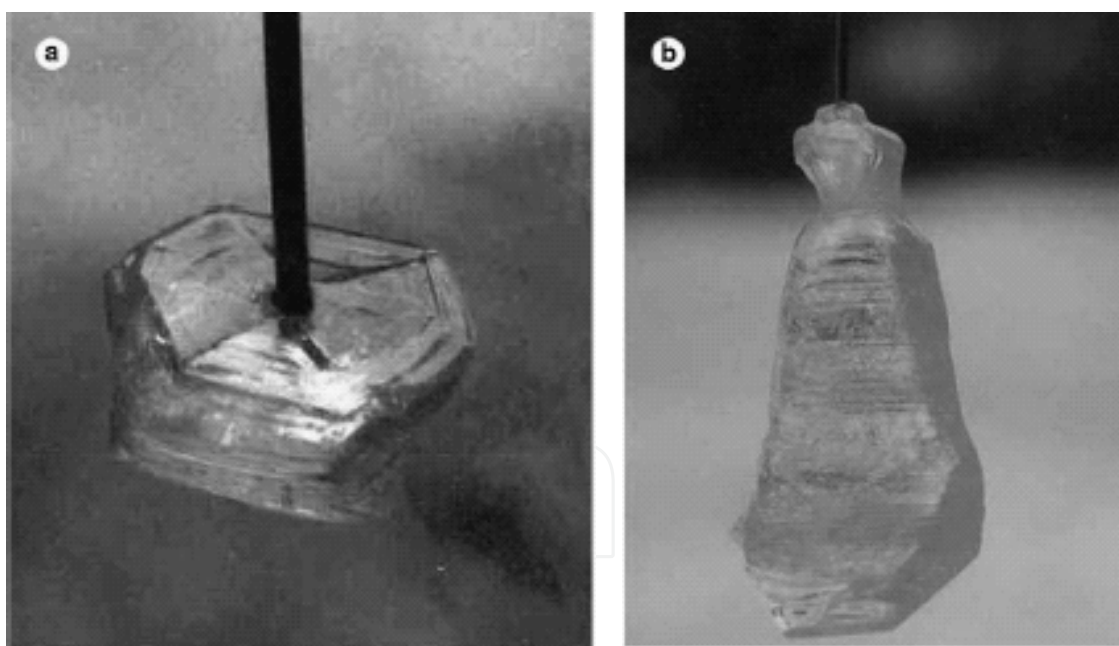


**Figure 5.** Photographs of the grown benzophenone crystals with (a) hexagonal morphology and (b) cubic morphology.

Further, the seed rotation rate plays a vital role in the initial stage of growth inside the microtube rather than during the growth. Sankaranarayanan et al (1998) [4] have reported that for a fixed radius of microtube there exists a critical rotation rate. Below this, the effect of change of crystal rotation is influential in deciding the morphology of the resultant crystal. If

the rotation rate is greater than the critical rotation rate, the effect of changes in rpm leads to very minimal effect since the radius of the microtube is very small. This has also been confirmed in the case of growth of benzophenone. Obvious change in morphology from hexagonal (Figure 5 a) to cubic (Figure 5 b) was observed by varying the seed rotation rate from 5 to 10 rpm at the initial stage of the growth [16].

Jackson et al has analyzed theoretically the structure of solid-liquid interfaces and has demonstrated that the morphology is determined by a factor ' $\alpha$ ' =  $(L_0/kT_e)(\eta/z)$  Where  $L_0$  = the enthalpy of fusion,  $k$ = Boltzmann's constant,  $T_e$ = equilibrium growth temperature,  $\eta$  and  $z$  are the number of atoms within the plane and the bulk crystal, respectively [17]. This analysis showed that materials for which  $\alpha > 2$  are generally faceted on one or more planes. Moreover, the  $\eta/z$  value depends on the crystal structure of a material. Benzophenone has large  $\alpha$  factor ( $\alpha=6.3$ ) and faceted growth is to be expected [18]. Therefore the observed two different morphologies are probably due to large value of Jackson's  $\alpha$  factor. In addition, in order to obtain crystal with morphology as in the conventional Czochralski technique, efforts were made to study the influence of shoulder angle by varying the growth rate just after seeding was conducted. The experimental growth parameters such as  $t_{ms} = 44^\circ\text{C}$ ,  $l_{ums} = 1.5$  mm and seed rotation rate = 10 rpm were kept constant. The pulling rate and the axial temperature gradient were varied in order to vary the growth rate. At the initial stage of seeding and growth, no marked changes were observed until the growth rate was kept at low. A sudden increase in the growth rate leads to higher shoulder angle as evidenced in the figure 6. The growth was continued until the crystal reaches a required size. Thereafter it was pulled at high pulling rate in order to detach the crystal from the melt surface and to analyze the shape of the solid-liquid interface. The solid-liquid interface was found to be concave towards melt which indicates the higher growth rate [19].



**Figure 6.** Grown crystal with high shoulder angle.

The morphology of the grown crystal was cubic. It suggested that in  $\mu$ T-CZ technique, the resultant orientation of the growing crystal will be decided by the orientation of the crystals which emerges out of the microtube, it largely depends on the  $t_{ms}$  and  $l_{ums}$ . Subsequently the sample (Figure 7) was fabricated from the grown crystal by cut and polishing for structural and optical characterization studies.

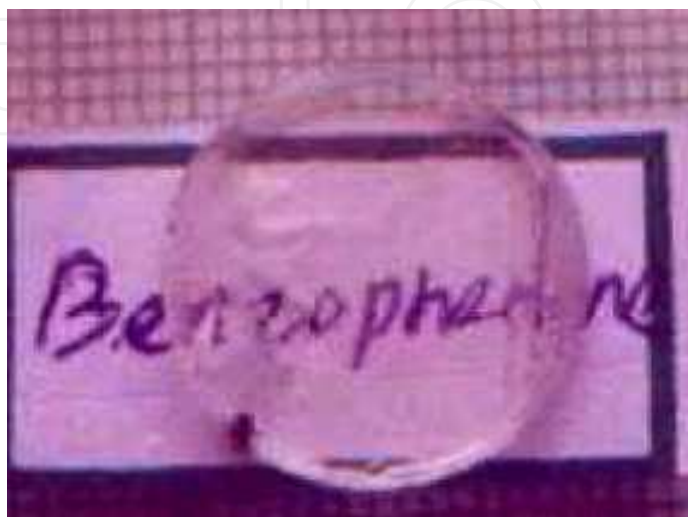


**Figure 7.** Prepared specimen from the  $\mu$ T-CZ grown crystal.

### 3.2.1. Orientation of the crystal

The nucleation phenomena that happened inside the microtube were explained with the aid of a schematic diagram in figure 8. In capillary rise, most of the organic melts form a convex meniscus. In Figures 8, 'a' and 'b' represent the melt level inside the microtube along both sides and this derivation mainly depends on the planarity of 'a' and 'b'. If the microtube exactly coincides with the center of axis of the system, then 'a' and 'b' lie at the same level. In that case, depending on the pulling rate of the microtube, a fine layer of melt will be retrieved along the wall due to wetting and nucleation will be initiated at 'a' and 'b', simultaneously. The axial temperature gradient and the cooling rate will influence the growth rate but the orientation at 'a' and 'b' need not be the same. If the orientation at 'a' and 'b' is the same (figure 8i), then the value of  $l_{ums}$  is not vital.

Suppose, the orientation of crystal is different at 'a' and 'b', then  $l_{ums}$  plays a crucial role. The value of  $l_{ums}$  should be sufficient enough to allow any one of the grains to proceed at the end of the microtube as the deciding crystal orientation. Since the radius of the microtube is very small, the value of  $l_{ums}$  will serve like the "necking" phenomena in melt crystal growth (Figure 8 ii). Owing to practical difficulties, if the microtube is deviated, i.e. as in figure 8 iii, it leads to differences in the thickness of the melt film retrieved. In this case, the resultant crystal orientation depends mainly on the orientation of the film which crystallized first (Figure 8 iv).

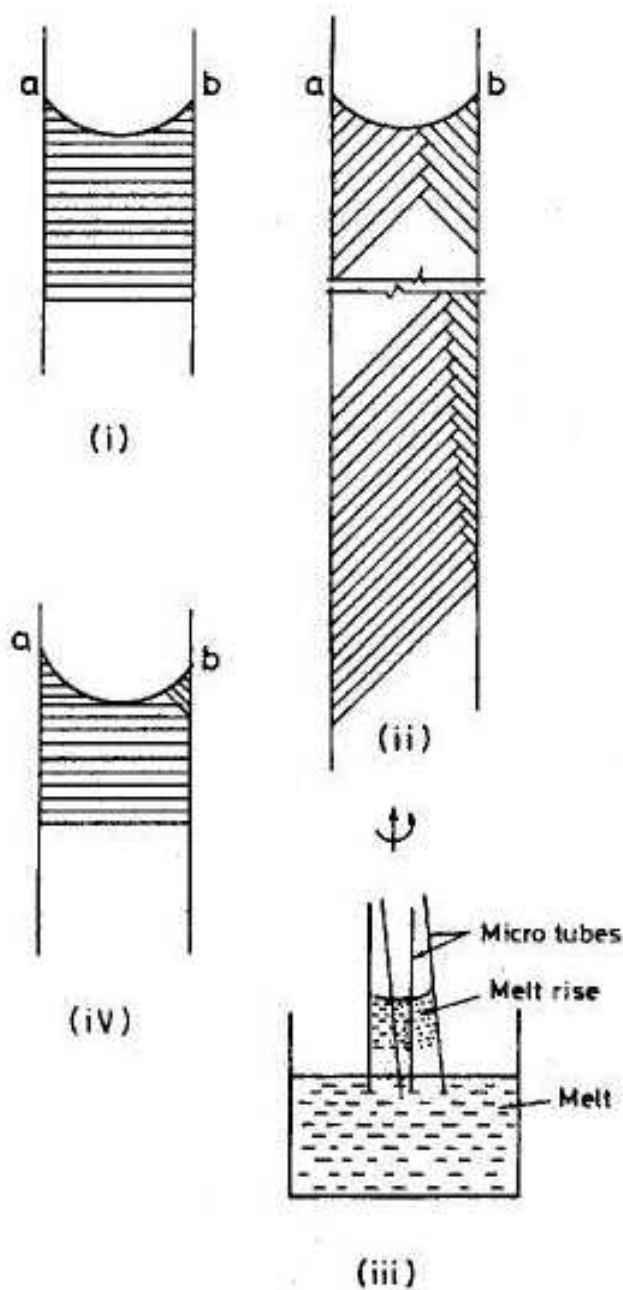


**Figure 8.** Schematic representation of initial growth of benzophenone inside the microtube.

Even though a crystal with multiple grains was formed inside the microtube initially, at the final stage of crystal growth inside the tube, a perfect single crystal was emerged out from the tube with single orientation facing the melt. The growth direction of the seed crystal was selected inside the microtube. Subsequently, the crystal at the middle part is grown like conventional Czochralski method with the seed crystal grown inside the microtube. Hence it would be possible to grow a single crystal with a particular orientation using a microtube.

### 3.3. USC growth

In this method, the effective zone width of the solution and the maximum temperature of the ring heater determine the effective evaporation rate of the solvent for a given diameter of the ampoule. Also, overheating the growth solution seems to be the key point to prevent spontaneous nucleation. Due to the transparent nature of the solution and the experimental set-up, real-time close-up observation on the solid-liquid interface was possible. The significant growth parameters of the USC technique are effective heating zone of solution column and temperature of the solution. Depending on the values of these two growth parameters, the solvent evaporation rate can be controlled more effectively. Moreover, the rate of supersaturation was controlled by means of controlling the solvent evaporation rate and thus the growth rate of the crystal can also be controlled. At an optimized growth conditions, maximum growth rate of 10 mm/day was achieved for the (110) orientation at 44°C of heating zone temperature. Cut and polished samples of USC grown crystal are shown in Figure 9.

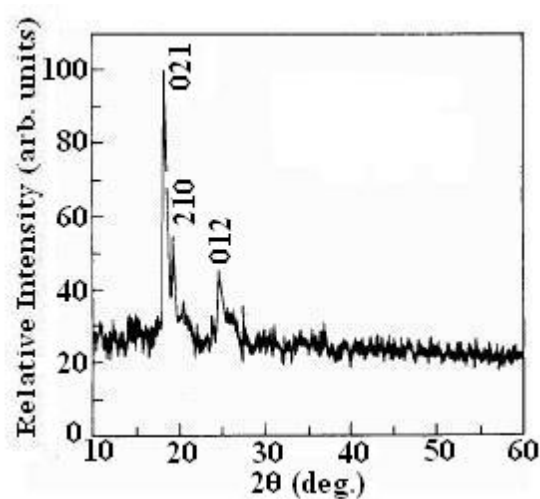


**Figure 9.** Cut and polished samples from USC grown crystal.

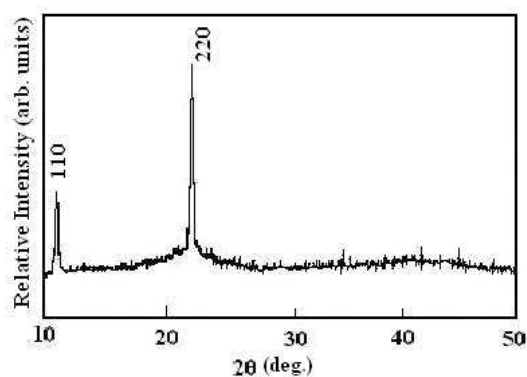
The grown ingots of benzophenone crystals by VB,  $\mu$ T-CZ and USC growth methods were characterized by XRD, HRXRD and LDT measurements and their results have been compared in the following sections.

### 3.4. X-ray diffraction (XRD) studies

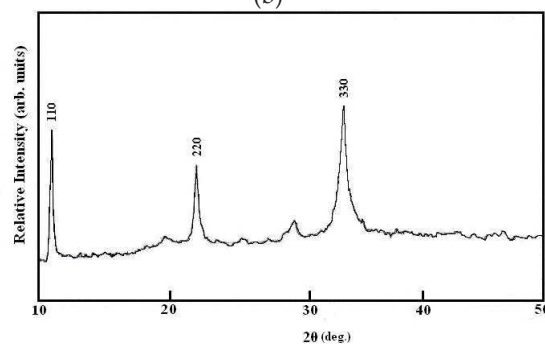
The ingots which were grown under optimized growth conditions using VB,  $\mu$ T-CZ and USC methods were subjected to X-ray diffraction studies. The cut and polished sample prepared from the grown ingots were used for XRD analysis to identify the growth orientation of the crystal. The XRD spectrums were recorded for the respective samples at room temperature in a  $2\theta$  range of 10 to 50° using  $\text{CuK}\alpha$  radiation of wavelength 1.5418 Å and the spectrums were shown in Figures 10 a, b, and c. From the diffraction pattern the d-spacing and hkl values for each diffraction peak in the corresponding spectrum of sample were identified. Using the orthorhombic crystallographic equation, the lattice parameter values of benzophenone were calculated and compared with the reported values [10]. The calculated values are in-line with the literature values.



(a)



(b)



(c)

**Figure 10.** X-ray diffraction spectrum recorded for benzophenone grown by (a) VB (b)  $\mu$ T-CZ and (c) USC method.

Moreover, in Figure 10 a, the presence of narrow and strongest peak along the  $\langle 021 \rangle$  direction confirms the single crystalline nature of the ingot grown by with VB  $\langle 021 \rangle$  as a most preferred orientation. In the case of  $\mu$ T-CZ grown crystal (Figure 10 b), the preferred orientation was along  $\langle 110 \rangle$  direction as evidence from the diffraction peaks at  $11.31^\circ$  and  $22.27^\circ$ . The obtained two different preferred orientations for a material grown from two different growth techniques demonstrate that the shape of the container material (tip of the ampoule in the case of VB growth, microtube in the case of microtube CZ growth) plays a vital role in the initial stage of nucleation. In unseeded crystal growth methods, the melt confinement in

a small volume will largely help to control over the formation and number of nucleation. The resultant orientation which emerges out of the tapered end (in the case of VB) or the microtube (in the case of  $\mu$ T-CZ) henceforth decides the growth orientation of the rest of the crystal. Even though spontaneous, multi nucleations were formed initially at both methods, it undergoes a geometric selection during the restricted growth inside the microtube/cone region of the ampoule. Therefore, it is quite feasible to grow a single crystal along a particular direction emerges out at the tapered end or at the end of the microtube if their physical length is sufficient to allow any one of the grain's orientation as a resultant growth direction. This happens when the progression of grains having low growth rate is suppressed or dominated by the progression of grain having the highest growth rate. Hence in the above two methods, it is possible to grow crystal along specific orientation by properly optimizing the growth conditions. In the case of USC method, the seed crystal was selected with the plane (110) as the imposing growth orientation. The recorded spectrum (Figure 10 c) on the grown sample justifies the unidirectional growth along the orientation of seed crystal.

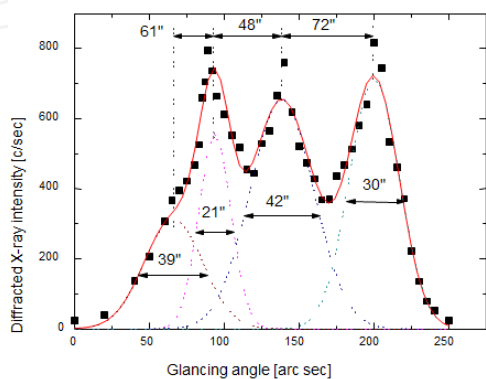
### 3.5. High-Resolution X-Ray Diffraction (HRXRD) studies

High resolution X-ray diffraction (HRXRD) studies have been carried out using multicrystal X-ray diffractometer (MCD) [20] on the grown samples to evaluate the crystalline perfection. A well-collimated and monochromated  $\text{MoK}\alpha_1$  beam obtained from a set of three plane (111) Si monochromator crystals set in dispersive (+,-,-) configuration has been used as the exploring X-ray beam. The specimen crystal was aligned in the (+,-,-,+) configuration. Due to dispersive configuration, though the lattice constant of the monochromator crystal(s) and the specimen are different, the unwanted dispersion broadening in the diffraction curve of the specimen crystal is considerably less.

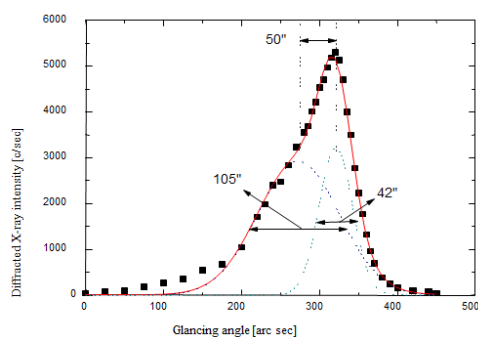
The HRXRD curves recorded by multicrystal X-ray diffractometer (MCD) revealed that the crystals grown by all the three methods contain internal structural grain boundaries. Figures 11 a and b show the diffraction curves (DC) recorded for the (211) diffracting planes of VB and  $\mu$ T-CZ grown sample using MCD with  $\text{MoK}\alpha_1$  radiation in symmetrical Bragg geometry. As can be seen from the Figure 11 a, the DC of the VB grown sample contains multiple peaks in an angular separation of few min., whereas the DC (Figure 11 b) of the  $\mu$ T-CZ grown sample contains only one additional peak at the angular separation of 50 arc sec. The DC of VB grown sample exhibits four main peaks with FWHM of 39, 21, 42 and 30 arc sec having angular separations 61, 48 and 72 arc sec. These multiple peaks illustrates that the samples contain many structural internal low angle ( $\alpha \geq 1$  arc min) grain boundaries, whose tilt angles range from 72 to 61 arc sec.

The DC (Figure 11 b) of  $\mu$ T-CZ grown sample shows that it contains two peaks, one main peak and the second peak at lower angle side, which indicates that the crystal contains a very low angle grain boundary ( $\alpha < 1$  arc min). The solid line in the figures is the convoluted curve obtained by the Gaussian fit of the observed peaks. The additional peak in the DC is 50 arc sec away from the main peak which corresponds to a very low angle grain boundary. The FWHM of the main peak and the second peak are respectively 42 and 105 arc sec. From this, one can infer that  $\mu$ T-CZ grown benzophenone crystal exhibited better crystalline quality than the VB grown crystal. Moreover, the presence of additional grains in VB grown

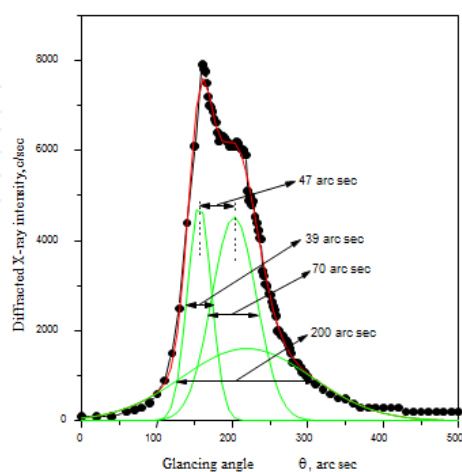
crystal was not found in  $\mu$ T-CZ grown crystal. The observation of the additional grain in VB grown crystal may be attributed to the differences in thermal expansion of the growing crystal and the ampoule which may lead to occurrence of plastic deformation in the grown crystal during post growth annealing process. Whereas such plastic deformations were absent in  $\mu$ T-CZ grown crystal due to the freestanding nature of the growing crystal. The HRXRD studies demonstrate that the microtube seeding is more reliable than VB growth for the growth of directional crystals with low imperfection.



(a)



(b)



(c)

**Figure 11.** HRXRD curve recorded for benzophenone grown by (a) VB (b)  $\mu$ T-CZ and (c) USC method.

The recorded DC (Figure 11 c) for the USC grown sample is considerably sharp but it contains two peaks: one main peak and second, a hump at higher angle side, which indicates that crystal contains a very low angle ( $\alpha < 1$  arc min) grain boundary. The solid line (convoluted curve) is well fitted with the experimental points represented by the filled circles. On deconvolution of the diffraction curve, it is found that there are three peaks. The two main peaks are separated by  $\sim 47$  arc sec and their half widths are 39 and 70 arc sec, respectively. The third peak is quite broad and having FWHM of 200 arc sec. All these three peaks were merged with the main peak and not possible to identify before deconvolution, which shows that the crystalline quality of the specimen is reasonably good. From the results, one can infer that the unidirectional benzophenone crystal grown by the USC method has relatively good crystalline perfection. The presence of the additional peaks may be attributed to the possible plastic deformation occurred during the restricted growth of the crystal inside the ampoule.

### 3.6. Laser damage threshold measurements

Optical damage in dielectric materials (NLO materials) may severely affect the performance of high power laser systems as well as the efficiency of the optical devices based on nonlinear processes. Hence, high damage threshold is a significant parameter for nonlinear optical crystal. Two main mechanisms that cause laser induced damage in the wide band gap dielectric materials are dielectric break down and thermal absorptions. The laser induced damage studies have been carried out for the VB,  $\mu$ T-CZ and USC grown samples under identical experimental conditions. The samples were carefully selected from the grown ingots with better quality and low dislocation densities. Then the samples were chemically polished using ethanol just prior to the LDT measurements. A Q-switched Nd:YAG laser operating at 1064 nm radiation was used. The laser was operated at the repetition rate of 10 kHz with the pulse width of 65 ns. For the LDT measurement 1.64 mm diameter beam was focused on the sample with a 10 cm focal length lens. The beam spot size on the sample was 0.51 mm. The multiple shots LDT measurements were made on the VB,  $\mu$ T-CZ and USC grown samples. The samples were irradiated at different spots on the same plane at similar experimental condition (wavelength – 1064 nm; repetition rate – 10 kHz; pulse width- 65 ns; beam diameter- 1.64 mm) and the damage pattern was observed using an optical microscope.

The measured LDT values of benzophenone samples grown by VB,  $\mu$ T-CZ and USC method are 2.3, 3.0 and 7.9 MW/cm<sup>2</sup>, respectively. As evidenced from HRXRD studies, the high value of LDT for SR grown sample can be attributed due to the high crystalline perfection when compared with that of VB and  $\mu$ T-CZ grown samples. The threshold for bulk laser damage is in principle a material dependent property and imperfections in a material are depends on the growth parameters which are subjected to control during the growth process. Furthermore, the LDT is a function of pulse duration, maximum pulse power, pulse wavelength, focal point radius, and in the case of multi shot experiments, repetition rate [21]. It is known that in the long-pulse regime ( $\tau > 100$  ps), the damage depends on the rate of thermal conduction by the crystal lattice and in the short-pulse regime ( $\tau < 100$  ps), the

dielectric breakdown and various nonlinear ionization mechanisms (multi-photon, avalanche multiplication) become dominant [22]. Hence, thermal effects become important for the nanoseconds and longer pulse widths. In the present multi shot experiments, relatively longer pulse width (65 ns) and high repetition rate of laser (10 kHz) were used and it may cause the low LDT for all the benzophenone samples. Wang et al [9] reported that the single-shot LDT of benzophenone crystal is 17.6 GW/cm<sup>2</sup> at the wavelength of 1064 nm while 39.5 GW/cm<sup>2</sup> at the wavelength of 532 nm. In the same laser parameters, the reported single-shot LDT of KDP, a well-known NLO crystal is 14 GW/cm<sup>2</sup> at the wavelength of 1064 nm and 17 GW/cm<sup>2</sup> at the wavelength of 532 nm [9]. Hence, it is obvious that benzophenone crystal has higher LDT than that of KDP crystal. The mechanical hardness of the materials also plays a vital role in LDT of the crystals grown in different crystallographic orientations [23]. In the next section, the hardness property of the benzophenone was correlated with the observed damage profile during laser damage threshold measurements.

## 4. Anisotropy of hardness and laser damage threshold

### 4.1. Unidirectional benzophenone in different orientation

USC method was extended to grow unidirectional benzophenone single crystals in three different crystallographic directions such as <110>, <010> and <001>. For this experiment, transparent single crystals obtained by slow evaporation method were used as a seed. To grow unidirectional benzophenone crystal along different crystallographic directions, three identical glass ampoules having inner diameter of 20 mm were carefully mounted with respective plane of the seeds by facing normal to the saturated solution of benzophenone. Saturated solution of benzophenone with pre-determined solute concentration was prepared using xylene as a solvent and carefully transferred into the growth ampoule. In this experiment, the solutions were not heated by ring heater to allow the natural evaporation of solvents. Growth was initiated at the seed crystal-solution interface when the supersaturation increased by evaporation of solvent from the solution. The transparent nature of the experimental set-up and the visible elevation of the solid-liquid interface measured at specific intervals facilitated the measurement of growth rate for the three different directions. The measured data are tabulated (table 1) in comparison with the relative growth rates of conventional solution grown and melt grown benzophenone crystals [24]. The grown ingots were sliced perpendicular to growth direction using in-house built wet-thread cutting machine. Figures 12 a and b show the grown crystals and sliced specimens of benzophenone in three different orientations. The samples were chemically polished on a polishing sheet using a mixture of acetone and xylene in the volume ratio 1:2.

Table 1 shows the relative growth rates for benzophenone crystal grown from different crystallographic directions in comparison with the relative growth rates of conventional solution grown and melt grown benzophenone crystals [24]. High growth rate was observed along <001> direction and low growth rate was observed along <110> direction. The observed relative growth rates vary drastically with growth directions and it follows the same tendency

with the relative growth rates for melt grown benzophenone [24]. On the other hand, the observed growth rates do not follow the reported growth rates for conventional solution grown benzophenone (toluene solvent) [24]. In conventional solution growth, the rate of diffusion of solute molecules or growth slice can be influenced by solvents. Due to the different vapor pressure of the solvents and the chemical environment (interacting between the solute and solvent) around the growing surface, growth rate can be changed by solvents. Moreover, the solvent in the present experiment and growth mechanism are entirely different from the conventional solution growth and under cooled melt growth.

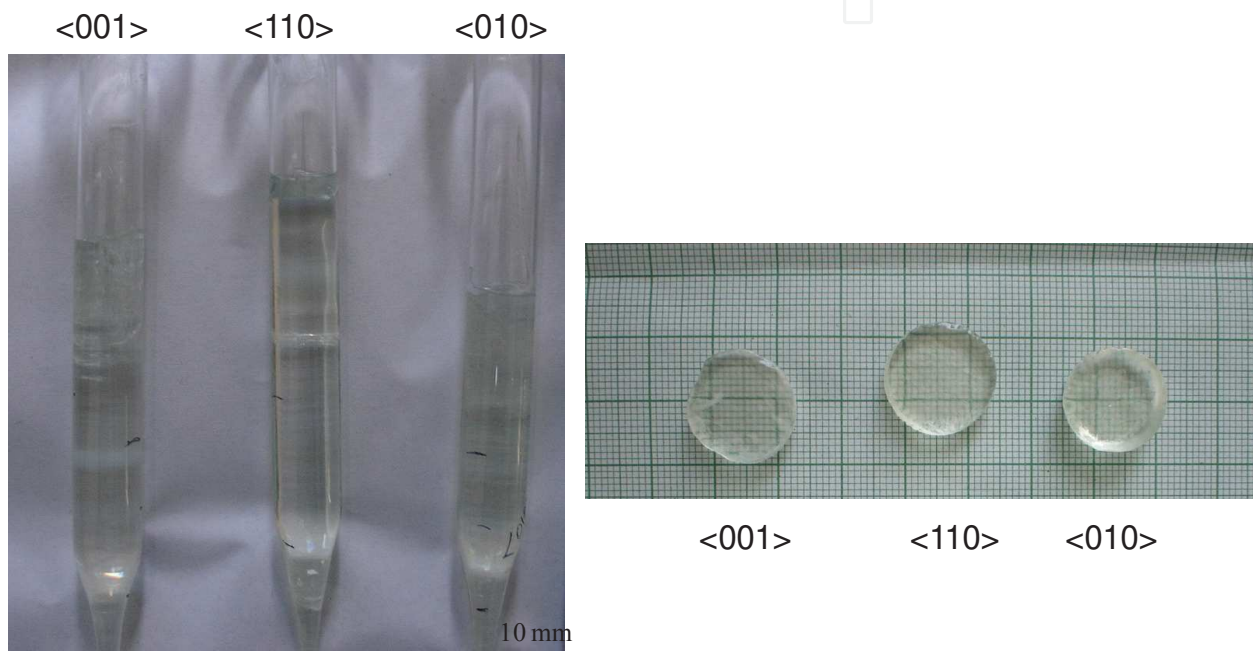


**Figure 12.** (a) Unidirectional benzophenone crystal in various growth directions and (b) prepared specimens from the respective ingots.

(hkl)	Uniaxial solution growth	Conventional solution growth (toluene solvent) [22]	Melt growth [22]
(110)	1.00	1.00	1.00
(010)	1.75	0.64	1.43
(001)	2.65	0.83	1.66

**Table 1.** Comparison between the relative growth rates of different growth directions for benzophenone crystals grown from conventional solution growth, melt growth [22], and uniaxial solution growth (this work). [The data are normalized with respect to the (110)]

In conventional solution growth, the growing crystal is fully exposed to the saturated mother solution. As a result, the crystal grows with different faces separated by growth sector boundaries. The shape of a crystal can be described by the distance from the centre of the crystal to the respective crystal faces and these distances are proportional to the relative growth rates of the crystal face [24]. The formation of inclusion in the growing crystal may cause the growth rate dispersions (GRD) [25, 26] i.e., a crystal (or crystal faces) of the same size growing under the same environmental conditions may grow at different rates. But, in USC method, unlike to conventional solution growth, the face (hkl) which has to grow is alone exposed to mother solution instead of the whole seed crystal. Hence the formation of inclusion due to solvent and other impurities incorporation is strongly suppressed in the present method. Moreover, in the USC grown crystals, the commonly observed growth features in the case of conventional solution grown crystal such as growth sector boundaries, twins, stacking faults and dislocations are not observed since the crystal was grown along selective growth axis [27].

The uniaxial crystallization process essentially involves gathering of a vast number of molecules together and forms a unique ordered arrangement which is driven by the level of supersaturation of the solution. The degree of supersaturation was controlled for all the experiments at predetermined solute concentration and constant temperature. The purity of the source materials and the solvent were almost the same for all the growth experiments. Hence, the observed variation in growth rate for different growth axis is likely to be the function of molecular packing energy or attachment energy,  $E_{att}$  of the respective growth face (eq (5)) [28].

$$R_{hkl} \propto E_{att} \quad (1)$$

$E_{att}$  can be defined as the energy released when one slice of thickness  $d_{hkl}$  crystallizes onto a crystal face (hkl). According to the BFDH model [29], the relative growth rate is inversely proportional to  $d_{hkl}$  (eq. (6)).

$$R_{hkl} \propto \frac{1}{d_{hkl}} \quad (2)$$

The reported attachment energy variation [29, 30] for the respective growth planes were compared with the growth rates and interplanar spacings ( $d_{hkl}$ ) (table 2). As shown in table 2, high growth rate was observed for the plane which has small  $d$  spacing and high attachment energy. However, the reported attachment energies were calculated by considering the conventional solution growth conditions [29] and undercooled melt growth conditions [30], that means it was considered that crystal grows in all faces simultaneously. In contrast, in the present experiment, the crystal has grown only on the selected growth face. Moreover, the different between the  $d$  spacing of (110) and (010) is very small (table 2). But the  $d$ -spacing for (001) plane is obviously smaller than other planes and has high growth rates compared to other planes.

(hkl)	Relative growth rates	Interplanar spacing d (hkl) (Å)	Attachment energy E <sub>att</sub> (kcal/mol)
(110)	1.00	7.82 (110)	10.3 <sup>a</sup> (9.86 <sup>b</sup> )
(010)	1.75	8.15 (010)	14.6 <sup>a</sup> (18.92 <sup>b</sup> )
(001)	2.65	6.01 (001)	17.1 <sup>a</sup>

ote: <sup>a</sup>Ref. [27] <sup>b</sup>Ref. [28]

**Table 2.** Comparison of relative growth rates of unidirectional crystals, d spacing (JCPDS data) and reported attachment energy for various growth directions.

#### 4.2. Optical absorption studies

The absorption coefficient of optical radiation in transparent materials is more vital in studies of the process of interaction of radiation with matter. The information on the energy absorbed by a material in the course of damage is an important characteristic to understand laser breakdown mechanism. In general, increase in the absorption is mainly due to the defects in the crystal and the presence of inclusions as well as impurities. For optical applications, the material considered must be highly transparent (low absorption) in the wavelength region of interest. The absorption coefficients of benzophenone are calculated using the following equations.

$$\alpha = -\frac{1}{d} \ln \frac{\left\{ [B^2 - R^2]^{\frac{1}{2}} - B \right\}}{R^2} \quad (3)$$

$$B = (1 - R^2) / 2T \quad (4)$$

$$R = \left( \frac{n-1}{n+1} \right)^2 \quad (5)$$

where d is the thickness of the crystal used for the optical studies and n is the refractive index of the crystal. T is the percentage of transmission and it was measured for 5 mm thick <110> oriented sample as a function of wavelength using UV-VIS-NIR spectrophotometer. The refractive index of the biaxial crystal (benzophenone) can be derived by the following equation:

$$n_{biaxial} = \frac{n_x + n_y + n_z}{3} \quad (6)$$

The reported refractive index data [8] for three different polarization of light parallel to a-axis ( $n_x$ ), b-axis ( $n_y$ ) and c-axis ( $n_z$ ) were used for the present calculations. The absorption coefficient curve of benzophenone is shown in Figure 13.

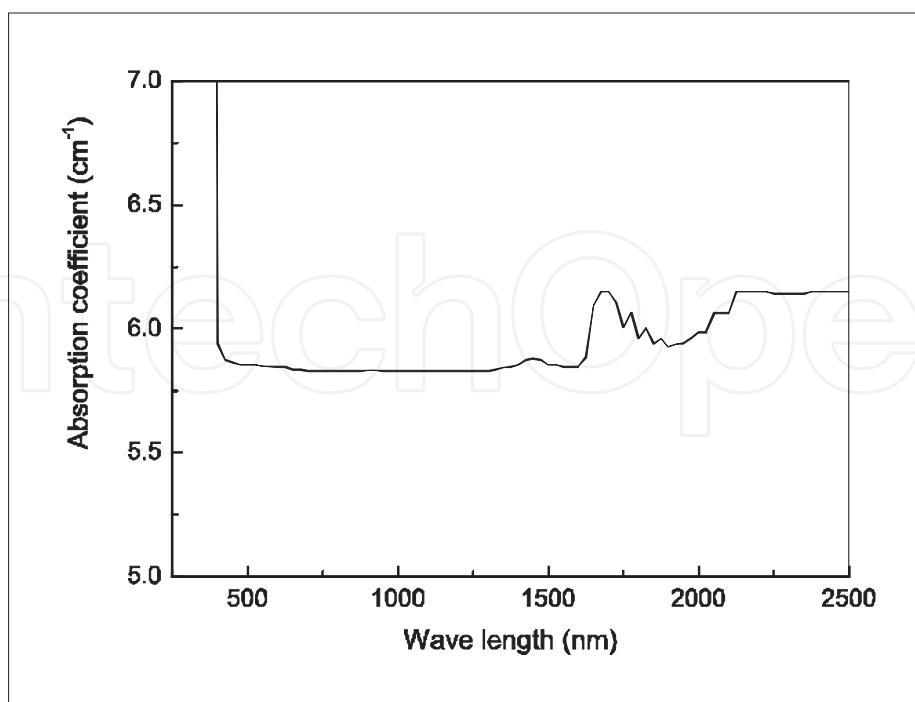


**Figure 13.** Measured absorption coefficients curve for benzophenone as a function of wavelength.

The presence of inclusion and grown-in defects (which can be controlled by growth process) causes the relative increase of absorption coefficient and thus increasing the over-all heating of the material during laser irradiation. The local heating in the region of an inclusion can lead to suppress the laser damage threshold value of a particular material. The present optical absorption study shows that the benzophenone material has very low absorption in the wavelength range from 400 to 1300 nm.

### 4.3. Micro hardness of benzophenone

Mechanical hardness of a material is also one of the decisive properties especially for post-growth processes and device fabrications. Load dependence of Vicker's micro hardness was measured on polished (110), (010) and (001) surfaces of 5 mm thick samples which were prepared from the respective unidirectional ingots. The indentation time was maintained as constant at 10 s. The diagonal lengths of the indented impression were measured for different loads varying from 10 to 80 g. The successive indentations were made at different sites of the sample surface. The mean diagonal length was used for the calculation of Vicker's hardness number (VHN). Figure 14 shows the VHN variation as a function of applied load for the (110), (010) and (001) planes of the prepared samples. Moreover, the mechanical hardness is correlated with the laser damage threshold of the materials. As can be seen from the Figure 14, the hardness number increased steeply in the beginning and got saturated after 50 g of load. Larger hardness value was measured for (010) plane whereas small hardness value was measured for (001) plane. The VHN values observed on (010), (110), (001) planes were 16.1, 14.6 and 12.8 at 60 g of load.

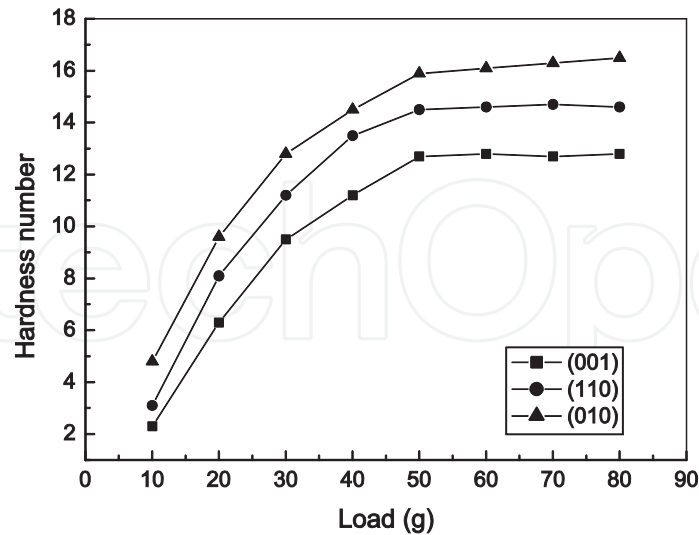


**Figure 14.** Hardness variation along three different crystallographic planes as a function of applied load.

#### 4.4. Laser damage threshold studies

The LDT was measured on the (110), (010) and (001) surfaces of the unidirectional crystals grown along the respective orientations. The samples used for LDT measurement were carefully selected from the grown ingots with best quality and low defect densities. Then the sample was chemically polished using xylene prior to the LDT measurements. A Q-switched Nd:YAG laser operating at 1064 nm radiation was used for single as well as multiple shot experiment. For the single shot experiment, the laser was operated at the repetition rate of 10 Hz with the pulse width of 10 ns. The single shot LDT measurements were made on the sample and the experiment was repeated at different places of each plane to measure the damage threshold precisely. During the single shot experiment, care was taken to select a fresh region after each shot to avoid the cumulative effects resulting from multiple exposures. For surface damage, the testing plane of the sample is placed at the focus point of the lens and the 50 mm diameter laser beam was focused on the sample using a lens of 20 cm focal length.

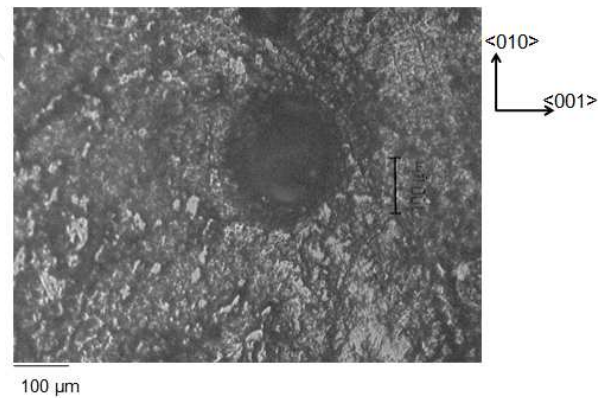
The surface damage can be determined by various methods, viz., by observing it with optical microscope, by visual incandescence, or by observing the scattering of helium-neon (He-Ne) laser beam passing through the damaged volume. In the present investigation, the resulting damage pattern is observed by an optical microscope. In order to observe the damage profile more clearly, the LDT experiment was performed on the (110) plane of the respective oriented ingot by multiple shots mode using the same laser with high repetition rate (10 kHz). Since the  $\langle 110 \rangle$  oriented ingot showed high micro hardness, it was selected for the multiple shot experiment. The sample was irradiated at different spots on the same plane at similar experimental condition and the damage profile was observed by optical microscope.

The respective single shot damage threshold measured for the  $\langle 110 \rangle$   $\langle 010 \rangle$   $\langle 001 \rangle$  oriented benzophenone samples was 16.99, 17.23 and 12.95 MW/cm<sup>2</sup> for 1064 nm Nd:YAG laser radiation. In the multiple shots experiment, the LDT value for (110) plane was measured as 7.69 MW/cm<sup>2</sup> using the 1064 nm Nd:YAG laser. For the single shot experiment, 1064 nm Nd:YAG laser with 10 ns of pulse width and 10 Hz of repetition rate was used. Whereas for the multiple shot experiment, the Nd:YAG laser with 65 ns of pulse width and 10 kHz of repetition rate was used. The threshold for bulk laser damage of a material mainly depends on laser parameters such as pulse width, focal spot geometry, and in the case of multi shot experiments, repetition rate of laser [21, 31]. From the single shot experiment, the anisotropic properties of the laser damage threshold were observed in the unidirectional benzophenone crystals. The  $\langle 010 \rangle$  oriented sample shows high laser damage threshold whereas the  $\langle 001 \rangle$  oriented sample shows low value of damage threshold. In both the case of single and multi shot experiments, due to large pulse width ( $\tau > 100$  ps) and low melting point of the material, thermal effects become the main causes for damage.

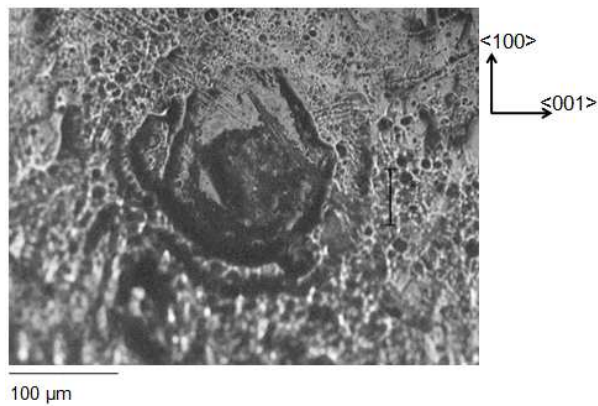
Figures 15 a, b and c show the optical micrograph of the single shot damage patterns for 1064 nm laser radiation on (110) (010) (100) planes of respective unidirectional benzophenone crystal. As can be seen from the Figure 15, irrespective of orientations, circular damage profile was obtained for all the samples at small repetition rate (10 Hz) and pulse width (10 ns). However, the diameter of the circular pattern was larger ( $\sim 1220$   $\mu\text{m}$ ) for  $\langle 001 \rangle$  oriented ingots whereas it was very small ( $\sim 200$   $\mu\text{m}$ ) in size for  $\langle 010 \rangle$  oriented ingot. Figure 16 shows the optical micrograph of the multiple shot damage pattern of 1064 nm laser radiation on (110) surface of unidirectional benzophenone crystal. The figure clearly depicts that the core of laser induced damage was at the centre of the pattern with strong cracks in different directions. As can be seen from Figure 16, the cracks were strongly propagated along the crystallographic  $\langle 001 \rangle$  and  $\langle 010 \rangle$  directions. It should be noted that the crack was stronger along  $\langle 001 \rangle$  direction compared to  $\langle 010 \rangle$  direction. Probably the high repetition rate and large pulse width causes the profound damage with cracks unlike to circular pattern observed in the single shot experiment.

Generally the hardness of the material is directly related to its bonding and crystallographic orientation. One can expect to obtain some information concerning the hardness anisotropy and damage profile observed in benzophenone based on its crystal structure. Benzophenone crystallizes in the non-centrosymmetric orthorhombic crystal structure with space group  $P2_12_12_1$  with four atoms per unit cell [9]. A projection of crystal structure along the c axis is shown in Figure 17 [30]. The shadowed elliptical chains disposed to each other at an angle of  $90^\circ$  show the rigid layers of the structures parallel to  $\langle 110 \rangle$  and  $\langle 101 \rangle$  directions and these directions correspond to predominant  $\{110\}$  prisms of the growth morphology of conventional solution grown crystal [32]. The strong bonding structure which forms rigid layers (shadows in Figure 17) causes higher mechanical hardness in (110) compared to (001) plane. Hence the size of the laser damage pattern was smaller for the ingot grown along  $\langle 110 \rangle$  direction (Figure 15 a) compared to the ingot grown along  $\langle 001 \rangle$  (Figure 15 c). On the other hand, when we look at the damage profile of the multi shot experiment (Figure 16) the cracks were strongly propagated along  $\langle 001 \rangle$  direction compared to  $\langle 010 \rangle$  direction. More-

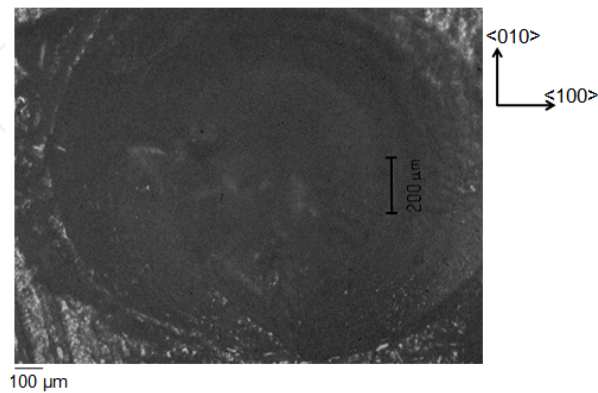
over, the intermolecular bonding energy of the respective growth plane plays a major role in hardness properties and laser induced damage. In addition, the magnitude of the cumulative bonding energy of a plane depends on the number of bonding of nearest neighbor of the atoms or molecules of the respective plane. From the hardness and damage profiles, it is obvious that the bonding energy of the (001) plane is small compared to (110) and (010) planes of benzophenone crystal. The intermolecular bonding energy can be related with the attachment energy as follows [28],



(a)



(b)



(c)

**Figure 15.** Optical micrograph of the damage pattern. (a) (110) surface, (b) (010) surface, (c) (001) surface.

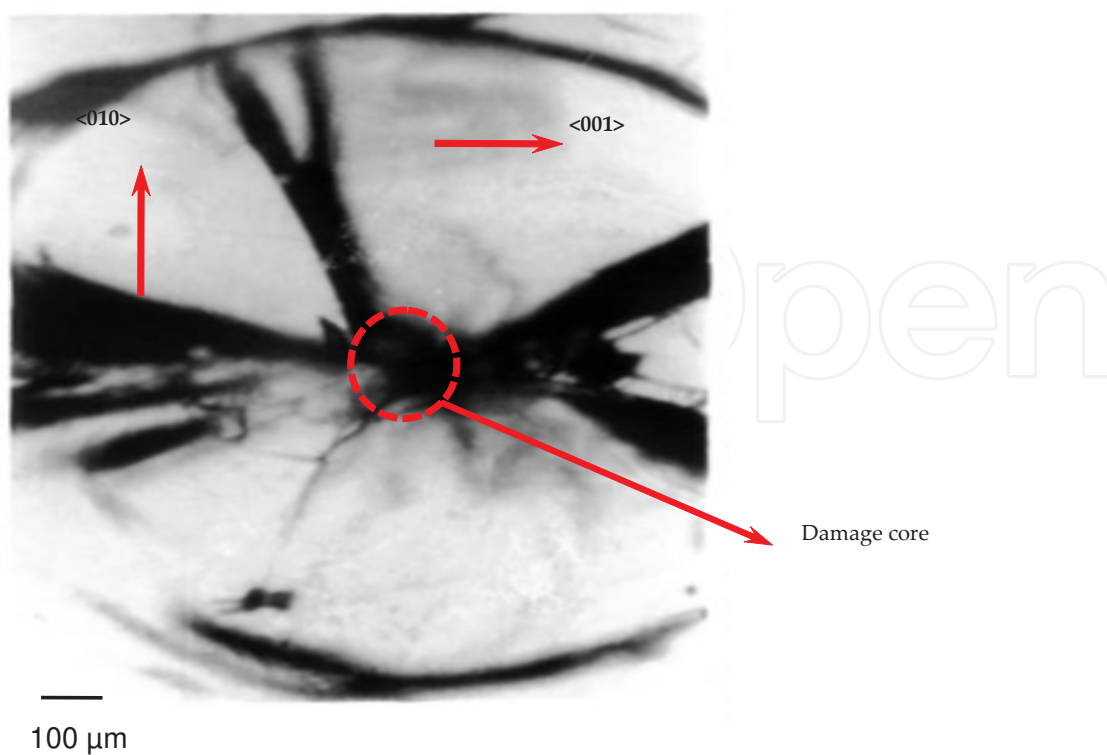


**Figure 16.** Optical micrograph of a damage pattern observed on the (110) surface for the laser with high repetition rate (10 kHz).

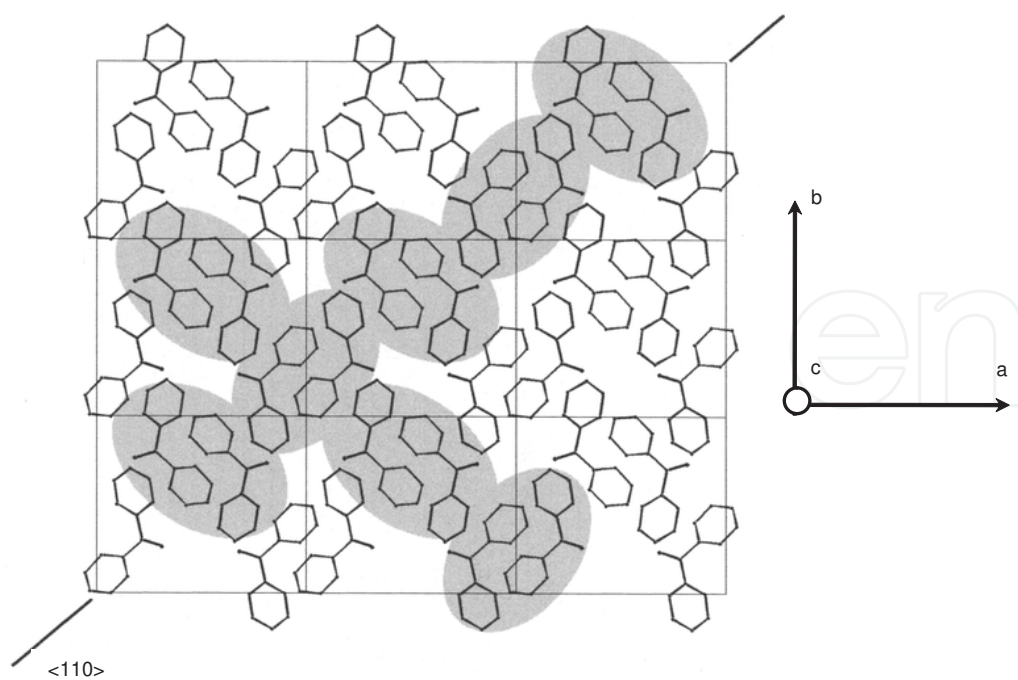


**Figure 17.** Molecular packing of benzophenone viewed on the orthorhombic (001) plane. The ridged layers parallel to <110> and <101> are shadowed.

$$E_{cry} = E_{sl} + E_{att} \quad (7)$$

Where  $E_{cry}$  is the crystallization energy or lattice energy and  $E_{sl}$  is the intermolecular bonding energy or slice energy of a growth plane.

According to the theory of Hartman and Bennema [28], the attachment energy is inversely proportional to the intermolecular bonding energy of the respective growth planes. In other words, a growth plane (hkl) which has low intermolecular bonding energy could grow with high growth rate and high attachment energy. As shown in table 2, the ingot grown from (001) plane had high growth rate and high attachment energy [29]. Moreover, small micro hardness value was measured on (001) plane and the size of the laser damage pattern was larger for the <001> oriented sample (Figure 15 c). This is probably because of weak intermolecular bonding existed in the (001) growth plane as high attachment energy was reported for the same plane of benzophenone crystal [29]. On the other hand, the ingot grown from (010) plane has low growth rate compared to ingot grown from (001) plane. High micro hardness value was measured on (010) plane and the size of the laser damage pattern was relatively small for the <010> oriented sample (Figure 15 b). In contrast, the ingot grown from (110) plane which has the lowest growth rate shows small micro hardness than that of ingots grown from (010) plane. It is feasible that the crystal is easily distorted in a line normal to the mechanical fragility, which results in a weak shearing stress of the crystal structure [21]. However, the relationship between the bonding energy of molecules and the shearing stress has not yet cleared well. In addition, the damage profile obtained for the <110> oriented sample under multi shot mode reveals some relation with the crack directions, hardness variations and crystallographic directions. As can be seen from Figure 16, a strong crack was observed along the mechanically weak <001> direction. Whereas the crack along <010> direction is quite weaker. From the results, it is obvious that the obtained damage profile is closed related with hardness anisotropy of the material.

## 5. Conclusion

Benzophenone single crystals were grown by various growth methods such as VB,  $\mu$ T-CZ and USC method and the structural perfection of the crystals were comparatively investigated. HRXRD studies revealed that the USC grown sample had relatively high crystalline perfection than the samples grown by other methods. On the other hand, VB grown crystal was found to have low crystalline perfection due to the difference in thermal expansion of the growing crystal and the ampoule which may lead to occurrence of plastic deformation in the grown crystal during post growth annealing process. The USC grown sample had high LDT than the crystals grown by other methods, probably due to low dislocation density in the USC grown ingots. Unidirectional benzophenone single crystals were grown along three different crystallographic directions. It was observed that the growth rate of the grown crystals varied with orientation. Moreover, the laser damage threshold was larger for the <110> and <010> oriented crystals compared to <001> oriented crystal at the wavelength of 1064 nm. The result was consistent with the hardness variation observed for the three different

crystallographic directions of benzophenone crystal. The optical micrographs of the damage profile and hardness anisotropy were correlated with the internal crystal structure of benzophenone.

## Author details

M. Arivanandhan<sup>1</sup>, V. Natarajan<sup>2</sup>, K. Sankaranarayanan<sup>3</sup> and Y. Hayakawa<sup>1</sup>

<sup>1</sup> Research Institute of Electronics, Shizuoka University, Hamamatsu, Japan

<sup>2</sup> Aditanar College of Arts and Science, Tirucherdur, Tamil Nadu, India

<sup>3</sup> School of Physics, Alagappa University, Karaikudi, Tamil Nadu, India

## References

- [1] Nakamura S, Senoh M, Nagahama S, Iwasa N, Yamada T, Matsushita T, Kiyoku H, and Sugimoto Y. InGaN Based Multi-Quantum-Well-Structure Laser Diodes. Japanese Journal of Applied Physics 1996; 35: 74–76.
- [2] Hollemann G, Peik E, and Walther H. Frequency-stabilized diode-pumped Nd:YAG laser at 946 nm with harmonics at 473 and 237 nm. Optical Letters 1994; 19: 192-194.
- [3] Yokoo A, Tomaru S, Yokohama I, Kobayashi H, Itoh H, Kaino T. A new growth method for long rod-like organic nonlinear optical crystals with phase-matched directions. Journal of Crystal Growth 1995; 156: 279-284.
- [4] Sankaranarayanan K, Ramasamy P. Microtube-Czochralski technique: a novel way of seeding the melt to grow bulk single crystal. Journal of Crystal Growth 1998; 193: 252-256.
- [5] Wang W, Huang W, Ma Y, Zhao J. Oriented growth of benzophenone crystals from undercooled melts. Journal of Crystal Growth 2004; 270: 469-474.
- [6] Arivanandhan M, Sankaranarayanan K, Ramamoorthy K, Sanjeeviraja C, Ramasamy P. A novel way of modifying the thermal gradient in Vertical Bridgman-Stockbarger Technique and studies on its effects on the growth of benzophenone single crystals. Crystal Research and Technology 2004; 39: 692-698.
- [7] Sankaranarayanan K, Ramasamy P. Unidirectional seeded single crystal growth from solution of benzophenone. Journal of Crystal Growth 2005; 280: 467-473.
- [8] Lammers D, Betzler K, Xue D, Zhao J. Optical Second Harmonic Generation in Benzophenone. Physica status solidi (a) 2000; 180: R5-R7.

- [9] Wang W, Lin X, Huang W. Optical properties of benzophenone single crystal grown from undercooled melt with oriented growth method. *Optical Materials* 2007; 29: 1063- 1065.
- [10] Masaru Tachibana, Shigeki Motomura, Akira Uedono, Qi Tang and Kenichi Kojima. Characterization of grown-in dislocations in Benzophenone single crystals by X-ray Topography. *Japanese Journal of Applied Physics* 1992; 31: 2202-2205.
- [11] Hammond R B, Pencheva K, Roberts K J. An examination of polymorphic stability and molecular conformational flexibility as a function of crystal size associated with the nucleation and growth of benzophenone. *Faraday Discuss* 2007; 136: 91-106.
- [12] Sekikawa T, Kosuge A, Kanai T, Watanabe, S. Nonlinear optics in the extreme ultraviolet. *Nature* 2004; 432: 605-608.
- [13] Carr C W, Radousky H B, Rubenchik A M, Feit M D, Demos S G. Localized Dynamics during Laser-Induced Damage in Optical Materials. *Physical Review Letters* 2004; 92: 087 401.
- [14] McArdle B J, Sherwood J N, Damask A C. The growth and perfection of phenanthrene single crystals: 1. Purification and single crystal growth. *Journal of Crystal Growth* 1994; 22: 193-200.
- [15] Arivanandhan M, Sankaranarayanan K, Ramasamy P. Studies on large uniaxially grown benzophenone single crystals. *Crystal Research and Technology* 2007; 42: 578-582.
- [16] Arivanandhan M, Sankaranarayanan K, Ramamoorthy K, Sanjeeviraja C, Ramasamy P. Microtube-Czochralski ( $\mu$ T-CZ) growth of bulk benzophenone single crystal for nonlinear optical applications. *Optical Materials* 2005; 27: 1864 -1868.
- [17] Jackson K A, Uhlmann D R, Hunt J D. On the nature of crystal growth from the melt. *Journal of Crystal Growth* 1967; 1: 1-36.
- [18] Bleay J, Hooper R M, Narang R S, Sherwood J N. The growth of single crystals of some organic compounds by Czochralski technique and the assessment of their perfection. *Journal of Crystal Growth* 1978; 43: 589-596.
- [19] Arivanandhan M, Sankaranarayanan K, Sanjeeviraja C, Arulchakkaravarthi A, Ramasamy P. Optical frequency doubling in microtube-Czochralski ( $\mu$ T-CZ) grown benzophenone single crystals. *Journal of Crystal Growth* 2005; 281:596-603.
- [20] Lal K, Bhagavannarayana G. A high resolution diffuse X-ray scattering study of defects in dislocation free silicon crystal grown by the floating zone method and comparison with Czochralski-grown crystal. *Journal of Applied Crystallography* 1989; 22: 209-215.
- [21] Yoshida H, Fujita H, Nakatsuka M, Yoshimura M, Sasaki T, Kamimura T, Yoshida K. Dependences of Laser-Induced Bulk Damage Threshold and Crack Patterns in Sever-

- al Nonlinear Crystals on Irradiation Direction. *Japanese Journal of Applied Physics* 2006; 45: 766-769.
- [22] Stuart B C, Feit M D, Rubenchik A M, Shore B W, Perry M D. Laser-Induced Damage in Dielectrics with Nanosecond to subpicosecond Pulses. *Physical Review Letters* 1995; 74: 2248-2251.
- [23] Vanishri S, Babu Reddy J N, Bhat H L, Ghosh S. Laser damage studies in nonlinear optical crystal sodium p-nitrophenolate dihydrate. *Applied Physics B: Lasers and Optics* 2007; 88: 457-461.
- [24] Roberts K J, Sherwood J N, Yoon C S. Understanding the Solvent-Induced Habit Modification of Benzophenone in Terms of Molecular Recognition at the Crystal/Solution Interface. *Chemistry of Materials* 1994; 6: 1099-1102.
- [25] Tanneberger U, Lacmann R, Herden A, Klapper H, Schmiemann D, Becker R A, Mersmann A, Zacher U. The dispersion of growth rate as a result of different crystal perfection. *Journal of Crystal Growth* 1996; 166: 1074-1077.
- [26] Ulrich J. Growth rate dispersion –a review. *Crystal Research and Technology* 1989; 24: 249-257.
- [27] Arivanandhan M Sankaranarayanan, K.; Ramasamy, P. Growth of longest <100> oriented benzophenone single crystal from solution at ambient temperature. *Journal of Crystal Growth* 2008; 310: 1493-1496.
- [28] Hartman P, Bennema P. The attachment energy as a habit controlling factor: I. Theoretical considerations. *Journal of Crystal Growth* 1980; 49: 145-156.
- [29] Roberts K J, Docherty R, Bennema P, Jetten L A M J. The Importance of considering growth-induced conformational change in predicting the morphology of benzophenone. *Journal of Physics D: Applied Physics* 1993; 26: B7-B21.
- [30] Wang W, Wang M, Huang W. Theoretical prediction and experimental study on the growth morphology of benzophenone crystals. *Materials Letters* 2005; 59: 1976-1979.
- [31] Yoshida H, Jitsuno T, Fujita H, Nakatsuka M, Yoshimura M, Sasaki T, Yoshida K. Investigation of bulk laser damage in KDP crystal as a function of laser irradiation direction, polarization, and wavelength. *Applied Physics B: Lasers and Optics* 2000; B70: 195-201.
- [32] Kutzke H, Klapper H, Hammond R B, Roberts K J. Metastable  $\beta$ -phase of benzophenone: independent structure determinations via X-ray powder diffraction and single crystal studies. *Acta Crystallographica B* 2000; B56: 486-496.

